



1 **Contrasting trends in element incorporation in hyaline and miliolid foraminifera**

2 Inge van Dijk¹, Lennart J. de Nooijer², Gert-Jan Reichart^{1,2}

3 ¹Department of Ocean Systems, NIOZ-Royal Netherlands Institute for Sea Research, Postbus 59, 1790
4 AB, Den Burg, the Netherlands, and Utrecht University.

5 ²Faculty of Geosciences, Earth Sciences Department, Utrecht University, Budapestlaan 4, 3584 CD,
6 Utrecht, the Netherlands

7

8 **Abstract**

9 We analyzed trends in element incorporation between hyaline (perforate) and miliolid (imperforate)
10 foraminifera in order to investigate processes involved in calcification affecting element incorporation
11 into foraminiferal carbonate. For both groups, we observed similar trends in element incorporation with
12 $p\text{CO}_2$, suggesting there some mechanisms to transports ions to the site of calcification are similar for
13 both calcification pathways, although the impact might be different across species. A previously
14 published trans-membrane transport model assumes foraminifera utilize Ca^{2+} channels to transport
15 calcium to the site of calcification. These channels are somewhat a-specific, leading to (accidental)
16 transport of other free ions. By modelling the activity of free ions as a function of $p\text{CO}_2$, we observed
17 that speciation of some elements (like Zn and Ba) are heavily influenced by the formation of carbonate
18 complexes. This leads to an increase in availability of free Zn and Ba with increasing $p\text{CO}_2$, which leads
19 to more transport to the site of calcification and subsequently incorporation in the foraminiferal shell.
20 We further observed that incorporation of the trace elements studied here is positively correlated
21 between the hyaline test building species. This could be due to dissimilar activity and/or selectivity of
22 calcium channels between species, perhaps due to differences in size. For miliolid calcification, part of
23 the calcium is obtained not only through channels but by also included seawater vesicles, which leads
24 to similar element to calcium ratios between species and element partitioning which is more in line with
25 inorganic carbonates.



26 1. Introduction

27 On the broadest taxonomic scale, calcareous foraminifera, cosmopolitan unicellular protists, produce
28 tests using either one of two fundamentally different mechanisms. These calcification strategies reflect
29 the evolutionary separation of foraminiferal groups dating back to the Cambrian diversification, from
30 where the imperforate miliolids and perforate hyaline foraminifera, developed independently
31 (Pawłowski et al., 2003). The calcification process of the latter group has been studied more extensively
32 than that of the miliolids (De Nooijer et al., 2014). Although many aspects of perforate calcification
33 remain unsolved, there is consensus that chamber formation takes place extracellularly, but within a
34 (semi-) enclosed space, generally termed the site of calcification (SOC). The first layers of calcite
35 precipitate on an organic matrix (the POS or primary organic sheet) that serves as a template for the
36 calcite layer that forms the chamber wall (Hemleben et al., 1977; Erez, 2003). To promote calcification,
37 foraminifera furthermore need to remove Mg ions and/or protons (Zeebe and Sanyal, 2002) from the
38 seawater entering the SOC. Many larger benthic foraminifera are hyaline species although the amount
39 of Mg in their shells is often more than 10 times higher than that of planktonic and small benthic hyaline
40 species, hence covering a large range in Mg/Ca values.

41 The calcification strategy of porcelaneous foraminifera is less well studied, which may be partly
42 explained by their limited application in paleoceanography. Porcelaneous foraminifera use a different
43 mode of calcification (Berthold, 1976; Hemleben et al., 1986; Debenay et al., 1998; De Nooijer et al.,
44 2009) and produce shells without pores (hence, the term imperforate) consisting of tablets or needles
45 (Debenay et al., 1998; Erez, 2003; Bentov and Erez, 2006). These calcitic needles (2-3µm) are
46 precipitated intracellularly (Berthold, 1976), after which they are transported out of the foraminifer to
47 form a new chamber (Angell, 1980). At the outer and inner layers of these chambers, the needles are
48 arranged along the same orientation so that they form an optically homogenous surface, giving it a shiny
49 (hence the term 'porcelaneous') appearance. In general the Mg/Ca values of the shells of porcelaneous
50 foraminifera are high.

51 Remarkably, despite this large biological control, incorporation of minor and trace elements still reflects
52 environmental conditions, in both hyaline and porcelaneous foraminiferal shells. For instance, the
53 Mg/Ca of foraminiferal shells is primarily determined by seawater temperature (Allen and Sanders,
54 1994; Nürnberg et al., 1996) and seawater Mg/Ca (Chapter 3; Segev and Erez, 2006; Evans et al., 2015;
55 Wit et al., in review). After correcting for the effect of the latter (if necessary) the use of foraminiferal
56 Mg/Ca has been validated by its wide application as paleothermometer (Elderfield and Ganssen, 2000;
57 Lear et al., 2000). Insight in vital effects (Erez, 2003) and inter-specific differences in trace element
58 incorporation (Bentov and Erez, 2006; Toyofuku et al., 2011; Wit et al., 2012) is needed for making the
59 Mg/Ca thermometer more robust. Systematic offsets between different species, interdependence of trace
60 elements incorporated (Langer et al., in press.) and the different response of element incorporation on



61 element speciation (Chapter 6; Keul et al., 2013; Wit et al., 2013), potentially provides useful clues for
62 determining which processes play an important role in the biomineralization pathways.

63 Here we present the results from a controlled growth experiment for which we used several
64 (intermediate- and high-Mg) hyaline and miliolid species and an inter-species comparison of trace
65 elements. We assessed the impact of bio-calcification on element incorporation as a function of $p\text{CO}_2$
66 in order to contrast the impact of different calcification strategies. During foraminiferal calcification,
67 incorporation of certain elements or fractionation of certain isotopes is shown to depend on the carbonate
68 system, e.g. $\text{U}/\text{Ca}_{\text{CALCITE}}$ (Russell et al., 2004; Keul et al., 2013) and $\text{Zn}/\text{Ca}_{\text{CALCITE}}$ to $[\text{CO}_3^{2-}]$ (Marchitto
69 et al., 2000; Chapter 6) and $\delta^{11}\text{B}$ to pH (Sanyal et al., 1996). Species-specific differences in partitioning
70 and fractionation most likely primarily reflect differences in calcification strategy. Offsets are largest
71 between hyaline and miliolid species, due to their fundamentally different calcification strategies (see
72 for a summary, Toyofuku et al., 2011). Differences in chemical composition and their dependency on
73 environmental variables can hence be used to identify key processes in miliolid and hyaline calcification.
74 We cultured eight benthic foraminiferal species (4 hyaline and 4 porcelaneous) under four different
75 $p\text{CO}_2$ conditions, analyzing incorporation of Mg, Sr, Na, Zn and Ba. Results are combined and compared
76 with literature data, to identify processes involved in calcification.

77

78 2. Methods

79 2.1 Foraminiferal collection

80 Large samples of macroalgae (*Dictyota* sp.) were collected in November 2015 at a depth of 2-3 meters
81 in Gallows Bay, St. Eustatius (N 17°28'31.6", W62°59'9.4"). Salinity was ~34 and temperature was
82 ~29°C at the site of collection. The collected macroalgae were transported to the laboratory at the
83 Caribbean Netherlands Science Institute (CNSI), where they were placed in a 5 L aquarium with aerated
84 and unfiltered seawater. From this stock, small amounts of algae and debris were gently sieved over a
85 90 and 600 μm mesh to carefully dislodge foraminifera. Several species of foraminifera were picked
86 from the resulting 90-600 μm fraction. Living specimens of *Marginopora vertebralis* (Quoy & Gaimard,
87 1830), *Amphistegina gibbosa* (d'Orbigny, 1839), *Laevipeneroplis bradyi* (Cushman, 1930) and *Archaias*
88 *angulatus* and limited amounts (<20) of *Peneroplis pertusus* (Forskål, 1775), *Asterigerina carinata*
89 (d'Orbigny, 1839), *Heterostegina antillarum* (d'Orbigny, 1839), and *Planorbulina acervalis* (Brady,
90 1884) characterized by yellow cytoplasm and pseudopodial activity, were selected for the culturing
91 experiments.

92

93 2.2 Culture set-up



94 We used an adapted version of the culture set-up described in Chapter 7. In short, four barrels each
95 containing 100 L of seawater (5 μ m filtered), were connected to a Li-Cor CO₂/H₂O analyzer (LI-7000),
96 to regulate the CO₂ level in the barrels' head space. The set levels were maintained by addition of CO₂
97 and/ or CO₂-scrubbed air according to the monitored *p*CO₂. The set-points for *p*CO₂ were 350 (A), 450
98 (B), 760 (C) and 1400 (D) resulting in four batches of seawater differing only in their inorganic carbon
99 chemistry. Salinity (34.0 \pm 0.2) was monitored with a salinometer (VWR CO310). The fluorescent
100 compound calcein (Bis[N,N-bis(carboxymethyl)aminomethyl]-fluorescein) was added to the culture
101 media (5 mg/L seawater) to enable determination of newly formed chambers during the culture
102 experiment (Bernhard et al., 2004). Short-term exposure (<three weeks) to calcein has no detectable
103 impact on the physiology of benthic foraminifera (Kurtarkar et al., 2015), and the presence of calcein
104 has no effect on the incorporation of Mg and Sr in foraminiferal calcite (Dissard et al., 2009). Culture
105 media was stored air-free in portions of 250 ml in Nalgene bottles with teflon lined caps at 4°C until
106 further use.

107 Foraminifera were divided over the different treatments in duplicate and placed in 70 ml Falcon[®] tissue
108 bottles with gas-tight caps in a thermostat set at 25°C (Fig. 1). The thermostat was monitored by a
109 temperature logger (Traceable Logger Trac, Maxi Thermal), monitoring the temperature every minute.
110 To create uniform light conditions, the thermostat was equipped with two LED shelves, which resulted in
111 high light conditions 12 hr/12hr. Culture media was replaced every four days, to avoid build-up of
112 organic waste and to obtain stable seawater element concentrations and carbon chemistry. Foraminifera
113 were fed after every water change with 0.5 ml of concentrated freeze-dried *Dunaliella salina* cells, pre-
114 diluted with the corresponding treatment seawater. After 21 days, the experiment was terminated.
115 Foraminifera were rinsed three times with de-ionized water, dried at 40°C and stored in
116 micropaleontology slides until further analysis at the Royal Netherlands Institute for Sea Research
117 (NIOZ).

118

119 **2.3 Analytical methods**

120 **2.3.1 Seawater carbon parameters**

121 At the start and termination of the experiment, 125 ml samples of the seawater at each of the different
122 experimental conditions were collected to analyze dissolved inorganic carbon (DIC) and total alkalinity
123 (TA) on a Versatile INstrument for the Determination of Titration Alkalinity (VINDTA) at the CNSI.
124 Using the measured DIC and TA values and the software CO2SYS v2.1, adapted to Excel by Pierrot et
125 al. (2006) the other carbon parameters (including [CO₃²⁻] and Ω_{calcite}) were calculated. For this we used
126 the equilibrium constants for K1 and K2 of Mehrbach et al. (1973), refitted by Dickson and Millero
127 (1987) (Table 1).



128

129 **2.3.2 Seawater element concentrations**

130 At the start and end of the experiment and during replacement of the culture media, subsamples were
131 collected in duplo using 50 ml LDPE Nalgene bottles and immediately frozen at -80°C . After
132 transportation to the NIOZ, melted samples were acidified with 3 times Quartz distilled HCl to pH ~ 1.8
133 and the seawater composition of the samples was analyzed on an Element 2 sector field double focusing
134 mass spectrometer (SF-ICP-MS) run in medium resolution mode. IAPSO Standard Seawater was used
135 as a drift monitor. Analytical precision (relative standard deviation) was 3% for Ca, 4% for Mg, 1% Na,
136 1% for Sr and 5% Ba. We obtained average values of 5.25 ± 0.06 mol/mol for Mg/Ca, 44.6 ± 0.6 mol/mol
137 Na/Ca, 8.63 ± 0.05 mol/mol for Sr/Ca, and 9.04 ± 0.47 for $\mu\text{mol/mol}$ Ba/Ca.

138 A subsample was analyzed using a commercially available pre-concentration system, SeaFAST S2.
139 With the SeaFAST system elements with low concentrations can be pre-concentrated to values above
140 detection limit of the SF-ICP-MS. Accordingly, we measured Cd, Pb U, B, Ti, Mn, Fe, Co, Ni, Cu, and
141 Zn. In short, 10ml of sample was mixed with an ammonium acetate buffer to pH 6.2 and loaded on a
142 column containing NOBIAS chelating agent. After rinsing the column with a diluted ammonium acetate
143 buffer the metals were eluted in 750 μl of quartz distilled 1.5 M HNO_3 before being quantified on the
144 SF-ICP-MS. Here we use the Zn data only, as this was analyzed in the foraminifera well. Analytical
145 precision (relative standard deviation) was 5% for Zn. We obtained average values 15.3 ± 0.5 $\mu\text{mol/mol}$
146 for Zn/Ca for all treatments. Although these values are clearly above natural open ocean values, the
147 concentrations are very uniform between treatments and when comparing start and end of the
148 experiments. The contamination with Zn might hence have occurred already when filling the culture
149 setup with the waters from the bay adjacent to the culture facility. In any concentrations are well below
150 values considered toxic (Nardelli et al., 2016).

151

152 **2.3.3 Cleaning methods**

153 After termination of the experiment, foraminiferal shells were cleaned following an adapted version of
154 Barker et al. (2003). Per treatment duplicate, all foraminifera were transferred to 10 ml PE vials. To each
155 vial, 10 mL 1% H_2O_2 solution (buffered with 0.5M NH_4OH) was added to remove organic matter. The
156 vials were heated for 10 minutes in a water bath at 95°C , and placed in an ultrasonic bath for 30 seconds
157 (degas mode, 80kHz, 50% power), after which the oxidizing reagent was removed. These steps (organic
158 removal procedure) were repeated five times. Foraminiferal samples were rinsed five times with
159 ultrapure water, after which the vials were stored overnight in a laminar flow cabinet at room
160 temperature to dry. Dried foraminifera were placed on double sided tape on LA-ICP-MS stubs. Pictures
161 were taken of individual foraminifera with a ZEISS Axioplan 2 fluorescence microscope equipped with



162 appropriate excitation and emission optics and a ZEISS Axiocam MRc 5 camera, to assess the number
163 of chambers added during the experiment based on the incorporation of calcein.

164

165 2.3.5. LA-ICP-MS

166 Element concentrations of individual fluorescent chambers were analyzed by Laser Ablation-ICP-MS
167 (Reichart et al., 2003; Van Dijk et al., in review). To determine foraminiferal element concentrations,
168 the laser system (NWR193UC, New Wave Research) at the Royal NIOZ was equipped with a 2-volume
169 cell 2 (New Wave Research), characterized by a wash-out time of 1.8 seconds (1% level) and hence
170 allowing detection of variability of obtained element to Ca ratios within chamber walls. Single chambers
171 were ablated in a helium environment using a circular laser spot with a diameter of 80 μm (*M.*
172 *vertebralis*) or 60 μm (other species). We ablated all calcein-stained chambers twice, except for the first
173 1-2 chambers that formed during the experiment to avoid contamination of calcite of chambers formed
174 prior to the experiments that may be overlapped by the first labelled chambers (Fig.2).

175 All foraminiferal samples were ablated with an energy density of $1\pm 0.1 \text{ J/cm}^2$ and a repetition rate of 6
176 Hz. The resulting aerosol was transported on a helium flow through an in house build smoothing device,
177 being mixed with a nitrogen flow (2 L/min), before entering the quadrupole ICP-MS (iCAP-Q, Thermo
178 Scientific). Monitored masses included ^7Li , ^{11}B , ^{23}Na , ^{24}Mg , ^{25}Mg , ^{27}Al , ^{43}Ca , ^{44}Ca , ^{66}Zn , ^{88}Sr and ^{137}Ba .
179 Contrary to ^{67}Zn and ^{68}Zn , ^{66}Zn is free of interferences when measuring calcium carbonate and SRM
180 NIST glass standards (Jochum et al., 2012). Potential contamination or diagenesis of the outer or inner
181 layer of calcite was excluded by monitoring the Al signal. At the start of each series, we analyzed SRM
182 NIST612 and NIST610 glass standard in triplicate (using an energy density of $5\pm 0.1 \text{ J/cm}^2$), JcT-1
183 (coral carbonate) and two in-house standards, namely NFHS (NIOZ Foraminifera House Standard;
184 Mezger et al., in review) and the Iceland spar NCHS (NIOZ Calcite House Standard). We further
185 analyzed JcP-1 (Giant clam) and MACS-3 (Synthetic Calcium Carbonate) at the start of each series,
186 and to monitor drift after every ten samples. All element to calcium ratios were calculated with an
187 adapted version of the MATLAB based program SILLS (Guillong et al., 2008). SILLS was modified to
188 evaluate LA-ICP-MS measurements on foraminifera, allowing import of Thermo Qtegra software
189 sample list, laser data reduction and laser LOG files. Major adaptations include improved automated
190 integration and evaluation of (calibration and monitor) standards, quality control report of the monitor
191 standards and export in element to calcium ratios (mol/mol). Calibration was performed against the
192 MACS-3 carbonate standard, with ^{43}Ca as an internal standard and we used the multiple measurements
193 of MACS-3 for a linear drift correction. Relative analytical precision (relative standard deviation (RSD)
194 of all MACS-3 analyses) is 3% for ^{23}Na , 3% for ^{24}Mg , 3% for ^{25}Mg , 4% for ^{66}Zn , 3% for ^{88}Sr and 3%
195 for ^{137}Ba . In total, 961 analyses were performed on 251 specimens covering eight species cultured in
196 four experimental conditions (see Table 2 for specifics).



197

198 We calculated the standard deviation (STD), RSD and standard error (STD/ \sqrt{n} ; SE) per treatment. The
199 partitioning coefficient (D) of an element (E) between seawater and foraminiferal calcite is expressed
200 as $D_E = (E/Ca_{\text{CALCITE}})/(E/Ca_{\text{SW}})$. Partition coefficients, element versus calcium ratio and growth
201 parameters were statistically compared with different experimental parameters (such as $p\text{CO}_2$ or $[\text{CO}_3^{2-}]$)
202 using a two-sided T-test with 95% confidence levels. This also allows for the calculation of 95%
203 confidence intervals over the average per treatment. Pairwise comparisons were made for per E/Ca per
204 species and culture conditions using ANOVA. Groups that showed significant difference were assigned
205 different letters. When comparing partition coefficients to other studies, E/Ca_{SW} data was, in some
206 studies, not measured. In these cases, we used average seawater E/Ca_{SW} to calculate D_E (see also
207 supplementary Table 1).

208

209 3. Results

210 3.1 Inter-species differences in element incorporation

211 In Table 3 we present all the elemental data for the eight species investigated in this controlled $p\text{CO}_2$
212 culture experiment. $\text{Mg}/\text{Ca}_{\text{CALCITE}}$ of Mg in hyaline species varies between 25.9-141.3 mmol/mol
213 Mg/Ca . In contrast, $\text{Mg}/\text{Ca}_{\text{CALCITE}}$ of miliolid species ranges from 121.3-149.3 mmol/mol. This large
214 spread in foraminifera E/Ca of hyaline species is also observed for Sr (1.7-3.1 mmol/mol), Na (3.4-19.5
215 mmol/mol), Zn (9.0-97.0 $\mu\text{mol}/\text{mol}$) and Ba (2.7-20.1 $\mu\text{mol}/\text{mol}$), while miliolids only vary over a
216 narrow range (Sr = 2.0-2.2 mmol/mol; Na = 3.8-5.8 mmol/mol; Zn = 53.0-140.8 $\mu\text{mol}/\text{mol}$; Ba = 18.0-
217 29.0 $\mu\text{mol}/\text{mol}$). When comparing Mg incorporation to that of the other elements studied here (Ba, Zn,
218 Sr and Na) between species (treatment B; Table 3), we observe a positive relation between D_{Sr}
219 ($p < 0.0025$), D_{Na} ($p < 0.0005$), D_{Ba} ($p < 0.05$) and D_{Zn} ($p < 0.005$) for hyaline species (Table 4). In general
220 hyaline species are enriched similarly in all elements (Fig. 3). Compared to porcelaneous species, the
221 hyaline shell building species which incorporate the most Mg (>100 mmol/mol Mg/Ca) incorporate
222 more Na, and Sr, while incorporating less Zn and Ba. Element incorporation across miliolid species is
223 less variable than observed for hyaline species and in general partition coefficients for these species
224 seem closer to inorganic values (Fig. 3). Including data from literature (both culture and field
225 calibrations; see supplementary Table S1), preferable in which both Mg/Ca and at least one other
226 element (Na, Sr, Ba or Zn) is measured, shows that the relation based on the Caribbean species studied
227 here is also more general applicable when including more species ($D_{\text{Sr}} = p < 0.005$; $D_{\text{Na}} = p < 0.0005$); D_{Ba}
228 = $p < 0.005$; $D_{\text{Zn}} = p < 0.01$), even though this compiled data (labeled 'All studies' in Table 4) covers a
229 wide range in environmental and experiment conditions.

230



231 3.2 Element/Ca as a function of ocean acidification

232 In both porcelaneous and hyaline species we find an increase of Zn/Ca_{CALCITE} and Ba/Ca_{CALCITE} with
233 *p*CO₂, while foraminiferal Sr/Ca, Mg/Ca and Na/Ca remain similar across the experimental conditions
234 (Fig. 4 and Table 5). Sensitivity of both foraminiferal Zn/Ca and Ba/Ca to changes in seawater *p*CO₂
235 differs between the studied porcelaneous and hyaline species. When *p*CO₂ changes from 350 to 1200
236 ppm, Zn/Ca of hyaline foraminifera increase by a factor of 3.7 (*A. carinata*) or 4.5 (*A. gibbosa*) while
237 miliolid foraminiferal Zn/Ca increases only by 1.3 (*M. vertebralis*), 1.8 (*A. angulatus*) and 2.1 (*L.*
238 *bradyi*). Also sensitivity of foraminiferal Ba/Ca to the same change in *p*CO₂ shows a similar pattern,
239 with Ba/Ca of hyaline species increasing by a factor of 3.6 (*A. carinata*) or 3.7 (*A. gibbosa*), while
240 miliolid species increase Ba/Ca only with a factor of 1.8 (*M. vertebralis*), 1.6 (*A. angulatus*) or 2.1 (*L.*
241 *bradyi*).

242

243 4. Discussion

244 4.1 Trends in element incorporation

245 Both miliolid and hyaline foraminifera promote calcification by increasing their internal pH (De Nooijer
246 et al., 2009). Still, they might use different mechanisms to take up the ions (Ca²⁺ and CO₃²⁻) necessary
247 for chamber formation, which is reflected in the different trends observed here. Element incorporation
248 in hyaline foraminifera is highly interdependent, i.e. species with increased Mg content also incorporate
249 more Sr, Na, Ba and Zn (Fig. 3). This observation suggests that uptake of all these elements is controlled
250 by the same process, which may be the transmembrane transport of calcium ions to the site of
251 calcification. Such transport likely involves Ca²⁺ channels (Nehrke et al., 2013), capable of transferring
252 other ions, like e.g. Mg, Sr and Na (Hess and Tsien, 1984; Allen and Sanders, 1994; Sather, 2005). This
253 may result in an interdependence between all these elements studied such as observed here for the
254 hyaline species if the selectivity for Ca²⁺ of these channels vary between species. In contrast, miliolid
255 species, building porcelaneous shells show much less inter-species variation in element incorporation
256 and ratios between incorporated elements is thus relatively similar between species (Fig. 3). This may
257 be explained by calcification from an internal reservoir, such as intracellular vacuoles containing
258 (modified) seawater (Hemleben et al., 1986; Erez, 2003). The fact that the Mg partitioning in this
259 foraminiferal group is similar to the inorganic partition coefficient may indicate that the carbonate is
260 directly precipitated from seawater, without major removal of Mg²⁺ ions. The relative similarity in
261 partition coefficients of other elements between miliolid species are generally in line with an inorganic-
262 like calcite precipitation, with only minor alteration of the elemental composition of the calcifying fluid
263 by ion channels.

264



265 4.2 Effect of ocean acidification on Element/Ca

266 For neither miliolid nor hyaline species, foraminiferal Mg/Ca, Na/Ca and Sr/Ca systematically change
267 with $p\text{CO}_2$. The impact of pH (and/or $[\text{CO}_3^{2-}]$) on Mg/Ca_{CALCITE} and Sr/Ca_{CALCITE} in foraminifera has
268 been the subject of discussion (e.g., Elderfield et al., 1996; Dissard et al., 2010). In low-Mg benthic
269 species, both Mg/Ca_{CALCITE} and Sr/Ca_{CALCITE} do not seem to depend on inorganic carbon system
270 parameters, e.g. pH or $[\text{CO}_3^{2-}]$ (Allison et al., 2011; Dueñas-Bohórquez et al., 2011). However, for
271 several planktonic species pH does influence Mg/Ca_{CALCITE} and Sr/Ca_{CALCITE} (Lea et al., 1999; Russell
272 et al., 2004; Evans et al., 2016). The effect of pH on Sr/Ca_{CALCITE} might be explained via increased
273 growth rates due to pH-associated changes in $[\text{CO}_3^{2-}]$ (Dissard et al., 2010). However, due to the limited
274 experimental set-up, we are not able to disentangle the effects of the different carbon parameters in this
275 study. Still, here we show that incorporation of Mg, Sr and Na of the selected larger benthic hyaline and
276 miliolid foraminifera are not significantly impacted when cultured over a range of $p\text{CO}_2$ and thus $[\text{CO}_3^{2-}]$
277 and pH values. Observed offsets in studies using acid titration (Lea et al., 1999; Russell et al., 2004;
278 Dueñas-Bohórquez et al., 2011; Evans et al., 2016) to alter the carbonate system might be related to
279 changes in alkalinity rather than $p\text{CO}_2$ or DIC. In the experimental setup here alkalinity was kept
280 constant between the different treatments, but pH, DIC and carbonate ion concentration varied as a
281 function of $p\text{CO}_2$.

282 In contrast, foraminiferal Zn/Ca and Ba/Ca are significantly impacted by $p\text{CO}_2$ for all species studied
283 here (Table 5; Fig. 4). Although Hönisch et al. (2011) suggested that the impact of carbonate chemistry
284 on Ba incorporation is negligible, their data does suggest a trend over the same interval in pH as studied
285 here. In hyaline foraminifera, Zn/Ca and Ba/Ca increases more as a function of $p\text{CO}_2$ (factor of 3.7-4.5
286 and 3.6-3.7, respectively when $p\text{CO}_2$ increases from 350 to 1200 ppm) compared to the miliolid species
287 (1.3-2.1 and 1.6-2.1 times, respectively). In the culture set-up used, increasing $p\text{CO}_2$ increases DIC,
288 reduces pH and thereby decreases seawater $[\text{CO}_3^{2-}]$. Speciation of Zn, Ba and also other elements, like
289 U (Keul et al., 2013), is primarily controlled by seawater $[\text{CO}_3^{2-}]$. Using the PHREEQC (Parkhurst and
290 Appelo, 1999) and the standard llnl database, the speciation of all elements studied here (Mg, Na, Sr,
291 Zn and Ba) for our different seawater treatments were modelled. We observed a decrease of free ions
292 (Zn^{2+} and Ba^{2+}) and an increase in Ba and Zn carbonate complexes (BaCO_3^0 and ZnCO_3^0), with
293 increasing $p\text{CO}_2$ (Fig. 5), while the activity of Mg^{2+} , Na^+ and Sr^{2+} remained unaffected. This suggests
294 that element incorporation in foraminiferal calcite might be depending on the bioavailability of free ions,
295 which in the case of Ba and Zn, changes with $p\text{CO}_2$.

296

297 4.3 Speciation in the foraminiferal microenvironment



298 During inorganic precipitation, carbonate complexes (e.g. MgCO_3^0) are easily incorporated into the
299 calcite crystal lattice. However, foraminifera build their test from ions available at the site of
300 calcification, which is well separated from the surrounding seawater (De Nooijer et al., 2009). During
301 calcification, Ca^{2+} is proposed to be transported from seawater to the SOC via ion channels (Nehrke et
302 al., 2013). This so-called trans-membrane transport (TMT) through Ca^{2+} channels has also been found
303 for other marine organisms, including coccolithophores (Gussone et al., 2006). These Ca^{2+} channels may
304 not discriminate perfectly between Ca ions and elements like Sr and Ba (Allen and Sanders, 1994),
305 causing accidental transport of these elements into the SOC. How much of a certain element will enter
306 the SOC in this way, depends on 1) the selectiveness of the channels and the characteristics of the
307 transported ions, 2) the element to calcium ratio in the foraminiferal microenvironment and 3) the
308 concentration gradient between seawater and the SOC. For instance, ions such as Mg^{2+} are heavily
309 fractionated against during TMT, which is reflected by the low D_{Mg} found in most species. The large
310 range in Mg/Ca values in hyaline species suggests that TMT plays an important, but also variable, role
311 in calcification of these species. The availability of some free ions, like Ba and Zn, changes as a function
312 of $p\text{CO}_2$ due to the formation of carbonate complexes (Fig. 5). When Zn and Ba form stable complexes
313 with carbonate ions they are no longer available for (sporadic) transport through the Ca^{2+} channels,
314 decreasing the availability at the site of calcification and subsequently, incorporation into the
315 foraminiferal calcite (Fig. 6).

316 In summary, the amount of Zn and Ba available at the site of calcification is proportional to the
317 concentration of the ratio between Ca^{2+} and free Zn^{2+} and Ba^{2+} in the foraminiferal microenvironment.
318 In turn, the amount of free Zn and Ba ions in seawater is controlled by their respective concentration in
319 seawater concentration, as well as $[\text{CO}_3^{2-}]$. Foraminiferal Mg/Ca, Na/Ca and Sr/Ca is not detectably
320 affected by $[\text{CO}_3^{2-}]$, since these elements do not form carbonate complexes over the range of $[\text{CO}_3^{2-}]$
321 studied here.

322

323 4.4 Element incorporation in hyaline species

324 Between hyaline species, we observe simultaneous increases in all elements incorporated and this trend
325 is confirmed when including published data for other species compiled from previous studies (Fig. 4
326 and supplementary Table S1). Interestingly, the two hyaline species that are most enriched in all
327 elements studied (Mg, Na, Sr, Zn and Ba) are also the foraminiferal species with the largest average
328 adult test size (*H. antillarum* and *P. acervalis*) for which data is available (this study). The other hyaline
329 species, *A. carinata* and *A. gibbosa*, have considerably smaller maximum shell sizes and lower Mg/Ca,
330 Sr/Ca, etc. values.



331 Two processes involving these calcium channels could possibly explain the observed size trend in
332 hyaline species. First, larger foraminifera have a smaller surface area to volume ratio and, therefore,
333 proportionally less Ca^{2+} channels, assuming the density of these channels per surface area remains
334 similar. This would imply that fewer channels need to transport more ions for a given volume of CaCO_3
335 precipitated, which may in turn, possibly reduce selectivity between Ca^{2+} and other divalent cations.
336 Secondly, a larger foraminifer will need more overall Ca^{2+} compared to smaller species for the
337 production of a single new chamber, since the volume of the chamber walls increases with the size of
338 the individual. This increased uptake of Ca^{2+} from the microenvironment around the foraminifer, may
339 cause a lower concentration of Ca^{2+} in the direct surroundings of the foraminifer compared to the other
340 ions, which may subsequently translate into an increased transport of ions other than Ca^{2+} to the site of
341 calcification.

342 A consequence of these hypotheses is that juvenile or smaller adults should have lower partition
343 coefficients than fully grown adults. Although some studies have shown a size effect for several
344 elements (e.g. Elderfield et al., 2002), other studies show no major effect of size on element partitioning
345 (e.g. Friedrich et al., 2012; Evans and Müller, 2013). The moderate trend observed within species, in
346 comparison to the large differences observed here between species, may indicate that species control
347 channel density per surface area as a function of average shell size of the species. Alternatively, the
348 maximum size of a species may be accompanied by a difference in their calcification mechanism (e.g.
349 the relative contribution of TMT in element uptake) explaining inter-species differences in element
350 partitioning. From an evolutionary point of view the latter explanation seems more likely.

351

352 **4.5 Mechanisms for element uptake in miliolid foraminifera**

353 In contrast to hyaline species, the miliolid species build porcelaneous shells that show much less inter-
354 species variation in element composition (Fig. 3). While hyaline species calcify in a (semi-)enclosed
355 space, miliolids precipitate their calcite intracellularly in vesicles in which they promote calcification
356 by increasing pH (De Nooijer et al., 2009). This suggests that these species calcify directly from seawater
357 (Ter Kuile and Erez, 1987). The fact that the Mg partitioning is close to the inorganic partition coefficient
358 in this foraminiferal group (Fig. 3) reflects that the carbonate is directly precipitated from intracellular
359 seawater, without major alteration of the original $[\text{Mg}^{2+}]$. The relative similarity in partition coefficients
360 between different porcelaneous shell building species is in line with primarily inorganic precipitation,
361 with only minor alteration of the elemental composition of the calcifying fluid by ion channels.

362 However, the observed correlation between $p\text{CO}_2$ and Ba and Zn (Fig. 4) suggests that Ca channels still
363 play a (modest) role in supplying Ca^{2+} to the miliolid SOC. The contribution of Ca^{2+} through TMT is
364 likely smaller than in hyaline species, since they already obtain calcium by including seawater in their



365 calcification vesicle prior to calcite precipitation. The considerably smaller flux of transmembrane Ca^{2+}
366 compared to perforate species explains the observed lower sensitivity of e.g. foraminiferal Zn/Ca and
367 Ba/Ca to changes in seawater $[\text{CO}_3^{2-}]$ in miliolid species (Fig. 4). This approximately 2 times lower
368 sensitivity of porcelaneous foraminifera compared to hyaline species suggests that miliolid foraminifera
369 acquire half of the necessary Ca^{2+} through Ca-channels, and the other half directly from vacuolized
370 seawater. Element incorporation in miliolid foraminifera will therefore be mainly governed by their
371 respective concentrations in seawater, and to a lesser extent by the selectivity for Ca^{2+} / permeability for
372 other ions during TMT.

373

374 5. Conclusions

375 Trends in element incorporation in larger benthic foraminifera can be explained by a combination of
376 differences in calcification strategy and seawater chemistry. Carbonate ion concentration in seawater
377 determines bioavailability of some ions (e.g. Zn^{2+} and Ba^{2+}), which are transported through Ca-channels
378 to the site of calcification. For hyaline foraminifera, we observed increased element incorporation for
379 larger species compared to smaller species, which can be explained by more intense activity of these
380 channels and the relative concentration in seawater during calcification. For miliolid foraminifera, only
381 half of the needed Ca is acquired through these Ca^{2+} channels, while the other half is obtained by
382 including small vesicles of seawater, leading to element partitioning to be more in line with inorganic
383 calcite.

384

385 Acknowledgments

386 This research is funded by the NIOZ – Royal Netherlands Institute for Sea Research and the Darwin
387 Centre for Biogeosciences project “*Double Trouble: Consequences of Ocean Acidification – Past,*
388 *Present and Future – Evolutionary changes in calcification mechanisms*” and the program of the
389 Netherlands Earth System Science Center (NESSC). Great thanks to all participants of the 2015
390 foraminifera culture expedition at the CNSI, St. Eustatia and Esmee Geerken for support with the salinity
391 culture experiment at the NIOZ. Furthermore, we would like to thank Kirsten Kooijman for supplying
392 *Dunaliella salina* cultures, Patrick Laan and Karel Bakker for seawater analysis and Mariëtte Wolthers
393 for providing technical support with PHREEQC. Lastly, we thank Jan-Berend Stuut (NIOZ) for the
394 usage of the Hitachi TM3000 SEM (NWO grant 822.01.008 and ERC grant 311152).

395



396 **References**

397

398 Allen, G.J. and Sanders, D. (1994) Two Voltage-Gated, Calcium Release Channels Coreside
399 in the Vacuolar Membrane of Broad Bean Guard Cells. *The Plant Cell* 6, 685-694.

400 Allison, N., Austin, H., Austin, W. and Paterson, D.M. (2011) Effects of seawater pH and
401 calcification rate on test Mg/Ca and Sr/Ca in cultured individuals of the benthic, calcitic
402 foraminifera *Elphidium williamsoni*. *Chemical Geology* 289, 171-178.

403 Angell, R.W. (1980) Test morphogenesis (chamber formation) in the foraminifer
404 *Spiroloculina hyalina* Schulze. *Journal of Foraminiferal Research* 10, 89-101.

405 Bentov, S. and Erez, J. (2006) Impact of biomineralization processes on the Mg content of
406 foraminiferal shells: A biological perspective. *Geochemistry, Geophysics, Geosystems* 7.

407 Bernhard, J.M., Blanks, J.K., Hintz, C.J. and Chandler, G.T. (2004) Use of the fluorescent
408 calcite marker calcein to label foraminiferal tests. *Journal of Foraminiferal Research* 34, 96-
409 101.

410 Berthold, W.-U. (1976) Biomineralisation bei milioliden Foraminiferen und die Matritzen-
411 Hypothese. *Naturwissenschaften* 63, 196-197.

412 Crocket, J.H. and Winchester, J.W. (1966) Coprecipitation of zinc with calcium carbonate.
413 *Geochimica et Cosmochimica Acta* 30, 1093-1109.

414 De Nooijer, L.J., Spero, H.J., Erez, J., Bijma, J. and Reichart, G.J. (2014) Biomineralization
415 in perforate foraminifera. *Earth-Science Reviews* 135, 48-58.

416 De Nooijer, L.J., Toyofuku, T. and Kitazato, H. (2009) Foraminifera promote calcification
417 by elevating their intracellular pH. *Proceedings of the National Academy of Sciences* 106,
418 15374-15378.

419 Debenay, J.-P., Guillou, J.-J., Geslin, E., Lesourd, M. and Redois, F. (1998) Processus de
420 cristallisation de plaquettes rhomboédriques à la surface d'un test porcelané de foraminifère
421 actuel. *Geobios* 31, 295-302.

422 Dickson, A.G. and Millero, F.J. (1987) A comparison of the equilibrium constants for the
423 dissociation of carbonic acid in seawater media. *Deep Sea Research Part A. Oceanographic*
424 *Research Papers* 34, 1733-1743.

425 Dissard, D., Nehrke, G., Reichart, G.J. and Bijma, J. (2010) Impact of seawater $p\text{CO}_2$ on
426 calcification and Mg/Ca and Sr/Ca ratios in benthic foraminifera calcite: results from culturing
427 experiments with *Ammonia tepida*. *Biogeosciences* 7, 81-93.



- 428 Dissard, D., Nehrke, G., Reichart, G.J., Nouet, J. and Bijma, J. (2009) Effect of the
429 fluorescent indicator calcein on Mg and Sr incorporation into foraminiferal calcite.
430 *Geochemistry, Geophysics, Geosystems* 10, n/a-n/a.
- 431 Dueñas-Bohórquez, A., Raitzsch, M., De Nooijer, L.J. and Reichart, G.-J. (2011)
432 Independent impacts of calcium and carbonate ion concentration on Mg and Sr incorporation
433 in cultured benthic foraminifera. *Marine Micropaleontology* 81, 122-130.
- 434 Elderfield, H., Bertram, C.J. and Erez, J. (1996) A biomineralization model for the
435 incorporation of trace elements into foraminiferal calcium carbonate. *Earth and Planetary
436 Science Letters* 142, 409-423.
- 437 Elderfield, H. and Ganssen, G. (2000) Past temperature and $\delta^{18}\text{O}$ of surface ocean waters
438 inferred from foraminiferal Mg/Ca ratios. *Nature* 405, 442-445.
- 439 Elderfield, H., Vautravers, M. and Cooper, M. (2002) The relationship between shell size
440 and Mg/Ca, Sr/Ca, $\delta^{18}\text{O}$, and $\delta^{13}\text{C}$ of species of planktonic foraminifera. *Geochemistry,
441 Geophysics, Geosystems* 3, 1-13.
- 442 Erez, J. (2003) The source of ions for biomineralization in foraminifera and their
443 implications for paleoceanographic proxies. *Reviews in Mineralogy and Geochemistry* 54, 115-
444 149.
- 445 Evans, D., Erez, J., Oron, S. and Müller, W. (2015) Mg/Ca-temperature and seawater-test
446 chemistry relationships in the shallow-dwelling large benthic foraminifera *Operculina
447 ammonoides*. *Geochimica et Cosmochimica Acta* 148, 325-342.
- 448 Evans, D. and Müller, W. (2013) LA-ICP-MS elemental imaging of complex discontinuous
449 carbonates: An example using large benthic foraminifera. *Journal of Analytical Atomic
450 Spectrometry* 28, 1039-1044.
- 451 Evans, D., Wade, B.S., Henehan, M., Erez, J. and Müller, W. (2016) Revisiting carbonate
452 chemistry controls on planktic foraminifera Mg/Ca: implications for sea surface temperature
453 and hydrology shifts over the Paleocene–Eocene Thermal Maximum and Eocene–Oligocene
454 transition. *Clim. Past* 12, 819-835.
- 455 Friedrich, O., Schiebel, R., Wilson, P.A., Weldeab, S., Beer, C.J., Cooper, M.J. and Fiebig,
456 J. (2012) Influence of test size, water depth, and ecology on Mg/Ca, Sr/Ca, $\delta^{18}\text{O}$ and $\delta^{13}\text{C}$ in
457 nine modern species of planktic foraminifers. *Earth and Planetary Science Letters* 319, 133-
458 145.
- 459 Guillong, M., Meier, D.L., Allan, M.M., Heinrich, C.A. and Yardley, B.W. (2008) SILLS:
460 A MATLAB-based program for the reduction of laser ablation ICP-MS data of homogeneous



461 materials and inclusions. Mineralogical Association of Canada Short Course Series 40, 328-
462 333.

463 Gussone, N., Langer, G., Thoms, S., Nehrke, G., Eisenhauer, A., Riebesell, U. and Wefer,
464 G. (2006) Cellular calcium pathways and isotope fractionation in *Emiliana huxleyi*. *Geology*
465 34, 625-628.

466 Hemleben, C., Be, A.W.H., Anderson, O.R. and Tuntivate, S. (1977) Test morphology,
467 organic layers and chamber formation of the planktonic foraminifer *Globorotalia menardii*
468 (d'Orbigny). *Journal of Foraminiferal Research* 7, 1-25.

469 Hemleben, C., Erson, O., Berthold, W. and Spindler, M. (1986) *fout*. *Biom mineralization in*
470 *lower plants and animals* (BSC Leadbeater, R Riding, eds) Clarendon Press, Oxford, 237-249.

471 Hess, P. and Tsien, R.W. (1984) Mechanism of ion permeation through calcium channels.
472 *Nature* 309, 453-456.

473 Hönisch, B., Allen, K.A., Russell, A.D., Eggins, S.M., Bijma, J., Spero, H.J., Lea, D.W. and
474 Yu, J. (2011) Planktic foraminifers as recorders of seawater Ba/Ca. *Marine Micropaleontology*
475 79, 52-57.

476 Ishikawa, M. and Ichikuni, M. (1984) Uptake of sodium and potassium by calcite. *Chemical*
477 *geology* 42, 137-146.

478 Jochum, K.P., Scholz, D., Stoll, B., Weis, U., Wilson, S.A., Yang, Q., Schwalb, A., Börner,
479 N., Jacob, D.E. and Andreae, M.O. (2012) Accurate trace element analysis of speleothems and
480 biogenic calcium carbonates by LA-ICP-MS. *Chemical Geology* 318–319, 31-44.

481 Keul, N., Langer, G., de Nooijer, L.J., Nehrke, G., Reichart, G.-J. and Bijma, J. (2013)
482 Incorporation of uranium in benthic foraminiferal calcite reflects seawater carbonate ion
483 concentration. *Geochemistry, Geophysics, Geosystems* 14, 102-111.

484 Kitano, Y., Okumura, M. and Idogaki, M. (1975) Incorporation of sodium, chloride and
485 sulfate with calcium carbonate. *GEOCHEMICAL JOURNAL* 9, 75-84.

486 Kurtarkar, S.R., Saraswat, R., Nigam, R., Banerjee, B., Mallick, R., Naik, D.K. and Singh,
487 D.P. (2015) Assessing the effect of calcein incorporation on physiological processes of benthic
488 foraminifera. *Marine Micropaleontology* 114, 36-45.

489 Lea, D.W., Mashiotto, T.A. and Spero, H.J. (1999) Controls on magnesium and strontium
490 uptake in planktonic foraminifera determined by live culturing. *Geochimica et Cosmochimica*
491 *Acta* 63, 2369-2379.

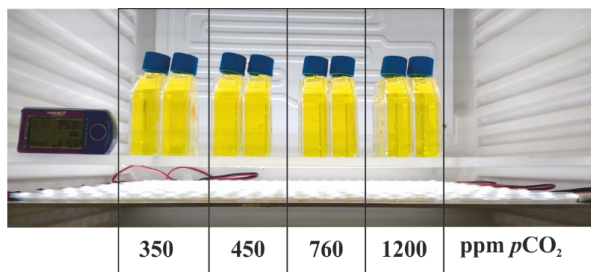
492 Lear, C.H., Elderfield, H. and Wilson, P.A. (2000) Cenozoic deep-Sea temperatures and
493 global ice volumes from Mg/Ca in benthic foraminiferal calcite. *Science* 287, 269-272.



- 494 Marchitto, T.M., Curry, W.B. and Oppo, D.W. (2000) Zinc concentrations in benthic
495 foraminifera reflect seawater chemistry. *Paleoceanography* 15, 299-306.
- 496 Mehrbach, C., Culbertson, C.H., Hawley, J.E. and Pytkowicz, R.M. (1973) Measurement of
497 the apparent dissociation constants of carbonic acid in seawater at atmospheric pressure.
498 *Limnology and Oceanography* 18, 897-907.
- 499 Mezger, E.M., de Nooijer, L.J., Boer, W., Brummer, G.J.A. and Reichart, G.-J. (in review)
500 Salinity controls on Na incorporation in Red Sea planktonic foraminifera. *Paleoceanography*.
- 501 Mucci, A. and Morse, J.W. (1983) The incorporation of Mg^{2+} and Sr^{2+} into calcite
502 overgrowths: influences of growth rate and solution composition. *Geochimica et*
503 *Cosmochimica Acta* 47, 217-233.
- 504 Nehrke, G., Keul, N., Langer, G., de Nooijer, L.J., Bijma, J. and Meibom, A. (2013) A new
505 model for biomineralization and trace-element signatures of Foraminifera tests. *Biogeosciences*
506 10, 6759-6767.
- 507 Nürnberg, D., Bijma, J. and Hemleben, C. (1996) Assessing the reliability of magnesium in
508 foraminiferal calcite as a proxy for water mass temperatures. *Geochimica et Cosmochimica*
509 *Acta* 60, 803-814.
- 510 Parkhurst, D.L. and Appelo, C. (1999) User's guide to PHREEQC (Version 2): A computer
511 program for speciation, batch-reaction, one-dimensional transport, and inverse geochemical
512 calculations. US Geol. Surv, Denver, Colorado.
- 513 Pawlowski, J., Holzmann, M., Berney, C., Fahrni, J., Gooday, A.J., Cedhagen, T., Habura,
514 A. and Bowser, S.S. (2003) The evolution of early Foraminifera. *Proc Natl Acad Sci U S A*
515 100, 11494-11498.
- 516 Pierrot, D., Lewis, E. and Wallace, D.W.R. (2006) MS Excel Program Developed for CO₂
517 System Calculations, ORNL/CDIAC-105a. Carbon Dioxide Information Analysis Center, Oak
518 Ridge National Laboratory, U.S.
- 519 Reichart, G.-J., Jorissen, F., Anschutz, P. and Mason, P.R. (2003) Single foraminiferal test
520 chemistry records the marine environment. *Geology* 31, 355-358.
- 521 Russell, A.D., Hönisch, B., Spero, H.J. and Lea, D.W. (2004) Effects of seawater carbonate
522 ion concentration and temperature on shell U, Mg, and Sr in cultured planktonic foraminifera.
523 *Geochimica et Cosmochimica Acta* 68, 4347-4361.
- 524 Sanyal, A., Hemming, N.G., Broecker, W.S., Lea, D.W., Spero, H.J. and Hanson, G.N.
525 (1996) Oceanic pH control on the boron isotopic composition of foraminifera: Evidence from
526 culture experiments. *Paleoceanography* 11, 513-517.

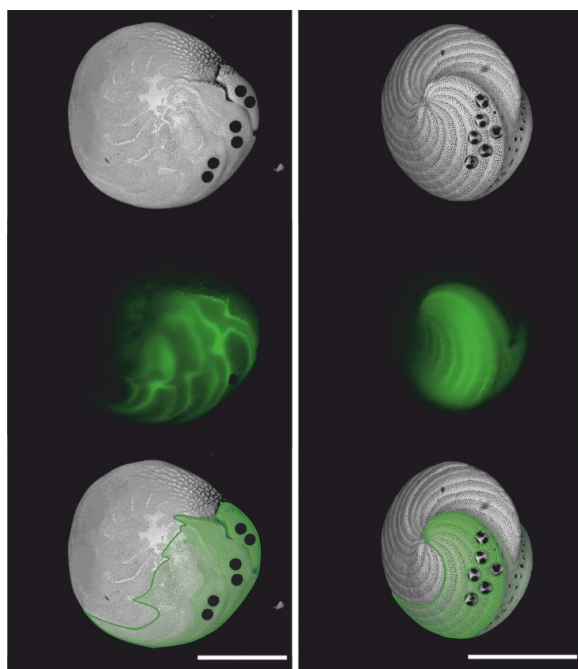


- 527 Sather, W.A. (2005) Selective Permeability of Voltage-Gated Calcium Channels, Voltage-
528 Gated Calcium Channels. Springer US, Boston, MA, pp. 205-218.
- 529 Segev, E. and Erez, J. (2006) Effect of Mg/Ca ratio in seawater on shell composition in
530 shallow benthic foraminifera. *Geochemistry, Geophysics, Geosystems* 7, n/a-n/a.
- 531 Ter Kuile, B. and Erez, J. (1987) Uptake of inorganic carbon and internal carbon cycling in
532 symbiont-bearing benthonic foraminifera. *Marine Biology* 94, 499-509.
- 533 Toyofuku, T., Suzuki, M., Suga, H., Sakai, S., Suzuki, A., Ishikawa, T., de Nooijer, L.J.,
534 Schiebel, R., Kawahata, H. and Kitazato, H. (2011) Mg/Ca and $\delta^{18}\text{O}$ in the brackish shallow-
535 water benthic foraminifer *Ammonia 'beccarii'*. *Marine Micropaleontology* 78, 113-120.
- 536 Van Dijk, I., de Nooijer, L.J., Wolthers, M. and Reichart, G.-J. (in review) Impacts of pH
537 and $[\text{CO}_3^{2-}]$ on the incorporation of Zn in foraminiferal calcite *Geochimica et Cosmochimica*
538 *Acta*).
- 539 Wit, J.C., de Nooijer, L.J., Barras, C., Jorissen, F.J. and Reichart, G.J. (2012) A reappraisal
540 of the vital effect in cultured benthic foraminifer *Bulimina marginata* on Mg/Ca values:
541 assessing temperature uncertainty relationships. *Biogeosciences* 9, 3693-3704.
- 542 Wit, J.C., de Nooijer, L.J., Wolthers, M. and Reichart, G.J. (2013) A novel salinity proxy
543 based on Na incorporation into foraminiferal calcite. *Biogeosciences* 10, 6375-6387.
- 544 Zeebe, R.E. and Sanyal, A. (2002) Comparison of two potential strategies of planktonic
545 foraminifera for house building: Mg^{2+} or H^+ removal? *Geochimica et Cosmochimica Acta* 66,
546 1159-1169.
- 547



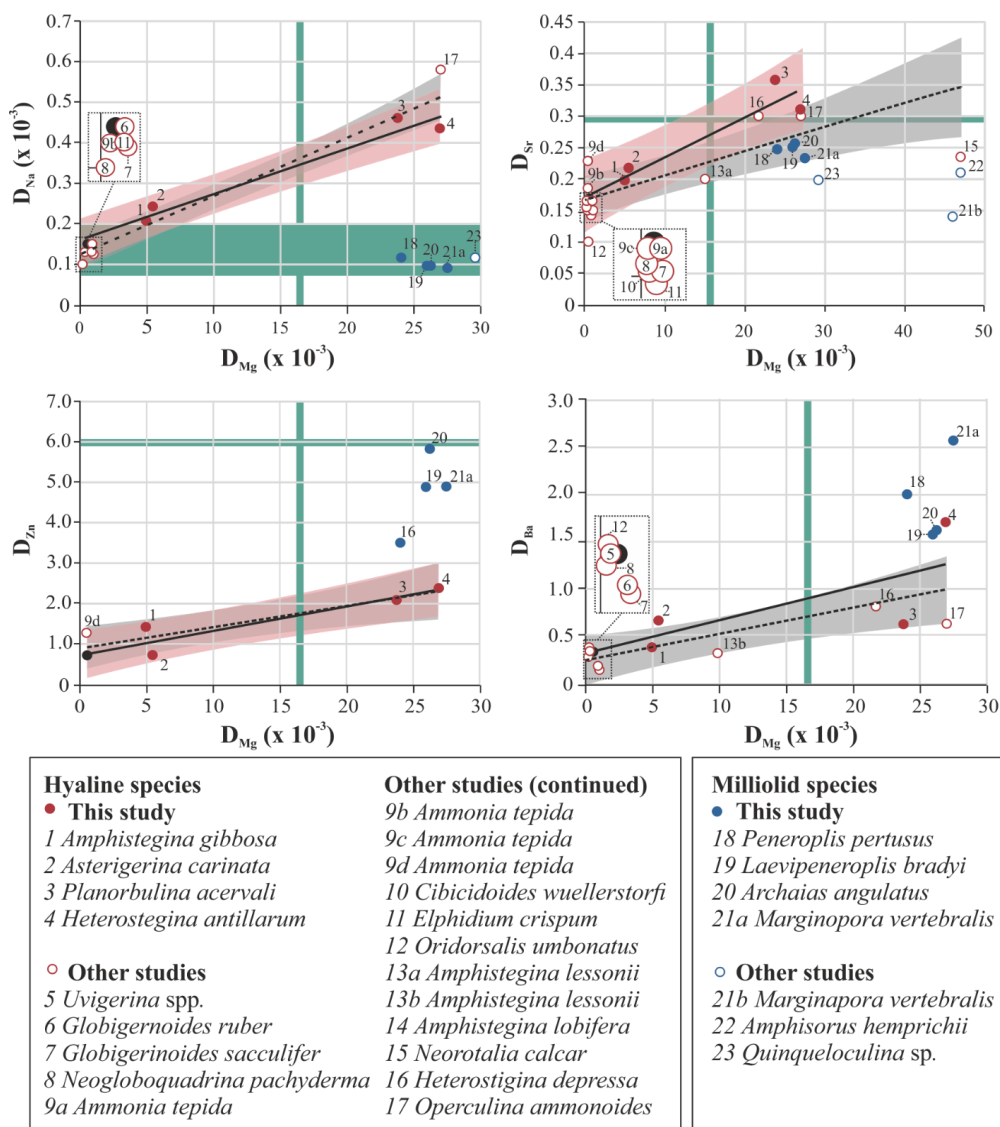
548

549 **Figure 1. Photograph of the culture set-up. Treatment with corresponding set-points are A=350,**
550 **B=450 ppm, C=760 ppm, D=1200 ppm.**



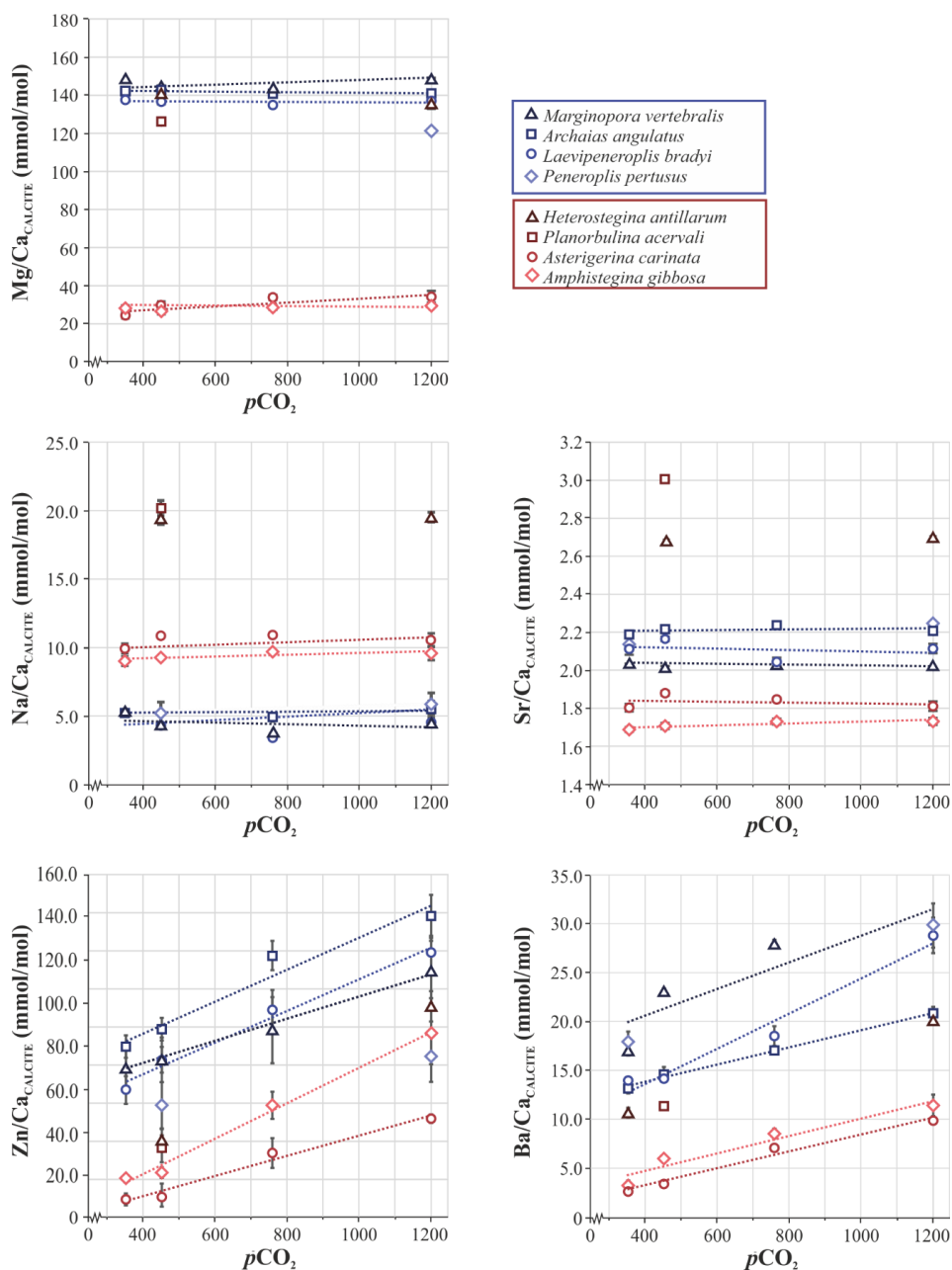
551

552 **Figure 2. SEM (top panels) and fluorescent microscope (middle panels) photographs of *A. gibbosa***
553 **(left) and *A. angulatus* (right) to assess newly formed chambers for laser ablation (lower panels).**
554 **Scalebars = 500 μ m.**



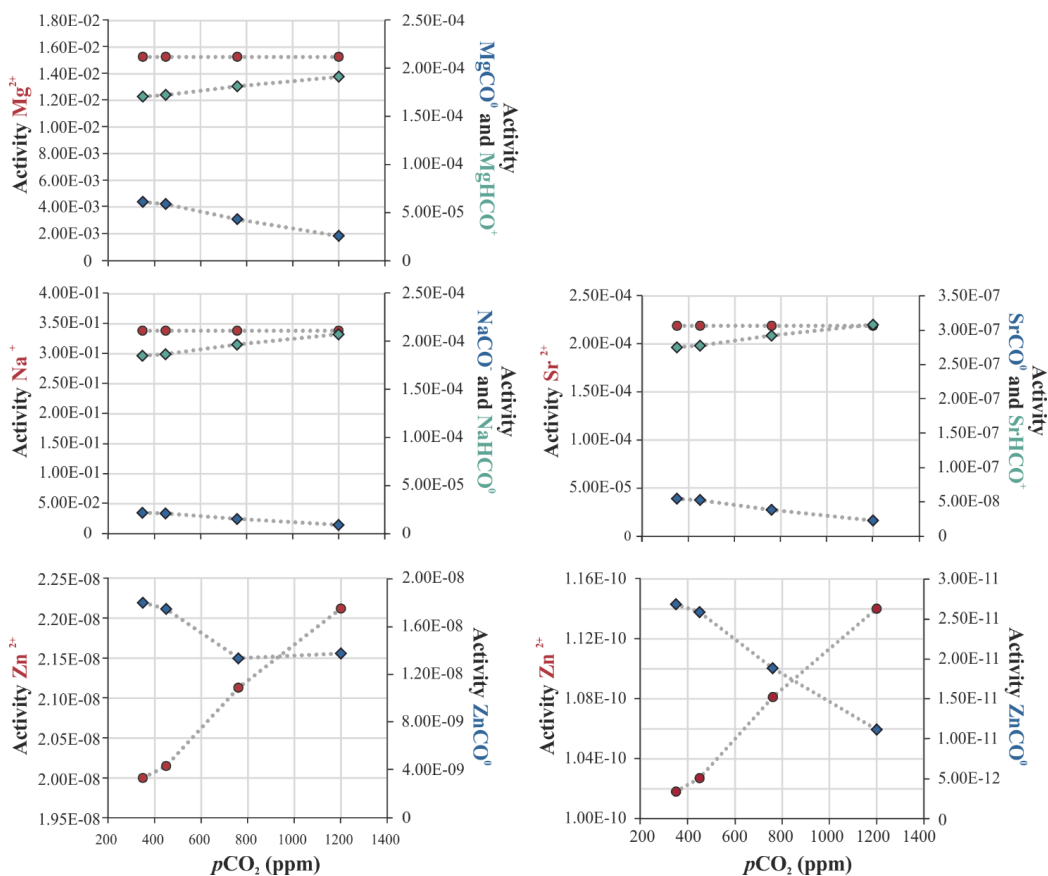
555

556 **Figure 3.** Partition coefficient of Na, Sr, Zn and Ba versus D_{Mg} of hyaline (red symbols) and
 557 miliolid (blue symbols) species in this study (closed symbols) and other studies (open symbols).
 558 Black lines represent trendlines (solid = this study; dashed = all studies). The 95% confidence
 559 intervals are indicated in pink (this study) and grey (all studies), which sometimes overlap. Black
 560 dots represent the NFHS, in-house carbonate standard, consisting of planktonic foraminifera. In
 561 green, inorganic partition coefficient from Mucci and Morse (1983), Ishikawa and Ichikuni (1984),
 562 Kitano et al. (1975) and Crocket and Winchester (1966). Numbers correspond to foraminiferal
 563 species analyzed (See supplementary Table S1)



564

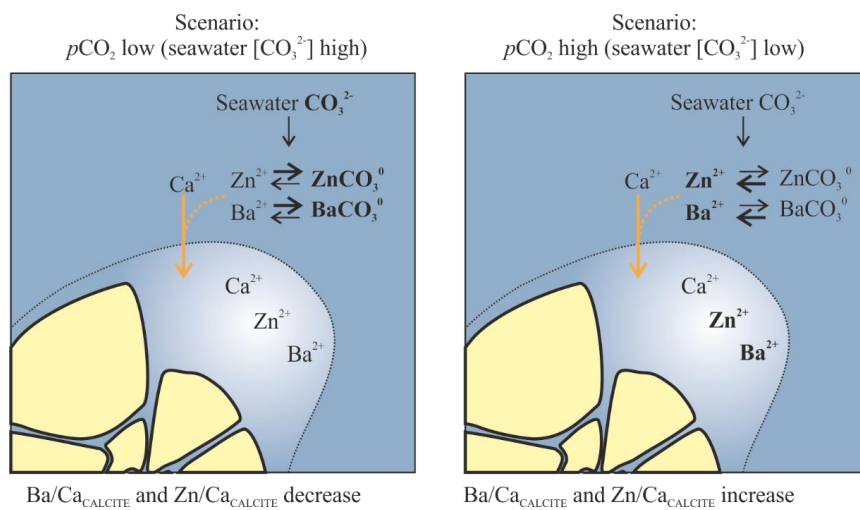
565 **Figure 4.** Element to Ca ratios (\pm SE) of different species of foraminifera over a range of $p\text{CO}_2$
 566 values. In some cases, the error bar is smaller than the symbol. Miliolid species in blue (triangles
 567 = *M. vertebralis*; squares = *A. angulatus*; circles = *L. bradyi*; squares = *P. pertusus*) and hyaline
 568 species in red (triangles = *H. antillarum*; squares = *P. acervali*; circles = *A. carinata*; diamonds =
 569 *A. gibbosa*).



570

571 **Figure 5. Speciation of Mg, Na, Sr, Zn and Ba in the different seawater treatments modelled in**
 572 **PHREEQC (Parkhurst and Appelo, 1999). Activities of free ions (red) and element (E)-carbonate**
 573 **complexes (ECO_3 = blue diamonds and EHCO_3 = green diamonds).**

574



576 **Figure 6. Schematic of incorporation of Zn and Ba during foraminiferal calcification under low**
577 **(left panel) and high (right panel) $p\text{CO}_2$ conditions. Amount of free ions (e.g. Zn^{2+} and Ba^{2+}) is**
578 **influenced by speciation due to changing $[\text{CO}_3^{2-}]$. Orange arrow indicates transport of Ca^{2+}**
579 **through channel, with the associated accidental transport of Zn^{2+} and Ba^{2+} .**
580



581 **Table 1. Carbon parameters (TA= Total alkalinity, n=2, DIC=Dissolved Inorganic Carbon, n=2)**
 582 **with (relative) standard deviation of the culture water per treatment of the $p\text{CO}_2$ experiment.**
 583 **CO2SYS was used to calculate seawater carbonate ion concentration, calcite saturation state and**
 584 **pH from measured TA and DIC.**

Treatment	Set-point	Measured		Calculated CO2SYS		
	$p\text{CO}_2$ ppm	TA $\mu\text{mol/kg}$	DIC $\mu\text{mol/kg}$	$[\text{CO}_3^{2-}]$ $\mu\text{mol/kg}$	pH (total scale)	Ω_{CALCITE}
A	350	2302.8±8.2	2007.5±10.7	211.2	8.04	5.1
B	450	2305.2±5.8	2021.3±12.5	204.1	8.02	4.9
C	760	2304.4±0.9	2100.8±13.4	153.3	7.86	3.7
D	1200	2300.3±0.7	2201.4±4.1	92.7	7.61	2.2

585



586 **Table 2. Total number of LA-ICP-MS measurements per species, per treatment (A-D).**

Species	n LA(n specimens)			
	A: 350 ppm	B: 450ppm	C:760 ppm	D:1200 ppm
<i>A. angulatus</i>	62(19)	72(21)	76(21)	51(14)
<i>M. vertebralis</i>	48(14)	49(15)	57(18)	33(11)
<i>A. gibbosa</i>	106(28)	126(32)	75(18)	59(15)
<i>L. bradyi</i>	21(5)	38(13)	27(5)	16(4)
<i>A. carinata</i>	12(2)	14(1)	19(4)	5(1)
<i>P. pertusus</i>		12 (2)		11 (2)
<i>H. antillarum</i>		12 (1)		14 (2)
<i>P. acervalis</i>		8 (2)		
Total	187(49)	331(87)	254(66)	189(49)

587



588 **Table 3. Overview of element to Ca ratios in foraminiferal calcite (Avg=average; SE=standard**
 589 **error) and partition coefficients D_E , with D_E of ambient conditions (treatment B) in bold. Letters**
 590 **(^a to ^d) indicate (per species per E/Ca) groups that are statistical different (one-way ANOVA).**

Species	pCO_2	Mg/Ca		Na/Ca		Sr/Ca		Zn/Ca		Ba/Ca	
		mmol/mol	D_{Mg} $\times 10^{-3}$	mmol/mol	D_{Na} $\times 10^{-3}$	mmol/mol	D_{Sr}	$\mu\text{mol/mol}$	D_{Zn}	$\mu\text{mol/mol}$	D_{Ba}
<i>A. angulatus</i>	350	139.4±0.6 ^a	26.6	5.2±0.1 ^a	0.12	2.2±0.02 ^a	0.25	80.0±5.1 ^a	5.3	13.2±0.5 ^a	1.5
	450	137.7±0.5 ^b	26.3	4.3±0.1 ^b	0.10	2.2±0.01 ^a	0.26	88.1±5.2 ^b	5.8	14.6±0.5 ^b	1.6
	760	137.4±0.7 ^b	26.2	4.9±0.1 ^c	0.11	2.2±0.01 ^a	0.26	122.6±7.0 ^c	8.1	17.0±0.6 ^b	1.9
	1200	138.6±1.1 ^a	26.4	5.4±0.2 ^a	0.12	2.2±0.02 ^a	0.26	140.8±9.9 ^d	9.3	20.9±0.2 ^c	2.3
<i>M. vertebralis</i>	350	147.7±0.6 ^a	28.2	4.8±0.1 ^a	0.11	2.0±0.01 ^a	0.24	70.0±10.1 ^a	4.6	17.0±0.5 ^a	1.9
	450	144.2±0.8 ^b	27.5	4.1±0.1 ^b	0.09	2.0±0.01 ^a	0.23	74.0±10.6 ^b	4.9	23.1±0.5 ^b	2.6
	760	143.0±0.6 ^a	27.3	3.8±0.1 ^a	0.09	2.0±0.01 ^a	0.23	87.7±15.5 ^c	5.8	27.9±0.6 ^c	3.1
	1200	148.3±0.5 ^b	28.3	4.5±0.2 ^c	0.10	2.0±0.01 ^a	0.23	115.6±15.3 ^d	7.6	30.1±0.2 ^d	3.3
<i>L. bradyi</i>	350	137.8±1.3 ^a	26.3	5.2±0.2 ^c	0.12	2.1±0.03 ^a	0.24	60.0±6.5 ^a	4.0	14.0±0.5 ^a	1.5
	450	136.2±0.7 ^a	26.0	4.3±0.1 ^b	0.10	2.2±0.01 ^b	0.25	73.8±6.0 ^b	4.9	14.2±0.5 ^a	1.6
	760	134.4±1.2 ^b	25.6	3.4±0.1 ^a	0.08	2.0±0.02 ^c	0.24	97.5±9.4 ^c	6.4	18.5±0.6 ^b	2.1
	1200	136.9±1.1 ^a	26.1	6.2±0.2 ^d	0.14	2.1±0.02 ^a	0.24	124.2±7.8 ^d	8.2	28.8±0.2 ^c	3.2
<i>P. pertusus</i>	350										
	450	126.1±1.8 ^a	24.0	5.2±0.3 ^a	0.12	2.1±0.07 ^a	0.25	53.0±10.8 ^a	3.5	18.0±0.5 ^a	2.0
	760										
	1200	121.3±1.0 ^a	23.1	5.8±0.2 ^a	0.13	2.2±0.02 ^a	0.26	75.5±11.9 ^b	5.0	29.8±0.2 ^b	3.3
<i>H. antillarum</i>	350										
	450	141.3±0.3 ^a	26.9	19.4±0.5 ^a	0.44	2.7±0.02 ^a	0.31	36.0±14.7 ^a	2.4	10.7±0.5 ^a	1.2
	760										
	1200	136.9±16 ^a	26.1	19.5±0.4 ^a	0.44	2.7±0.02 ^a	0.31	97.0±18.3 ^b	6.4	20.1±0.2 ^b	2.2
<i>P. acervalis</i>	350										
	450	139.1±1.2	26.5	19.5±0.7	0.44	3.1±0.02	0.36	31.6±6.6	2.1	11.3±0.5	1.3
	760										
	1200										
<i>A.</i>	350	23.6±1.5 ^a	4.5	9.9±0.4 ^a	0.22	1.8±0.02 ^a	0.21	9.0±2.6 ^a	0.6	3.2±0.5 ^a	0.4



	450	28.5±2.4 ^b	5.4	10.8±0.1 ^a	0.24	1.9±0.01 ^a	0.22	10.9±5.5 ^a	0.7	6.0±0.5 ^b	0.7
	760	33.1±1.2 ^b	6.3	10.9±0.2 ^a	0.24	1.8±0.01 ^a	0.21	30.7±7.0 ^b	2.0	8.5±0.6 ^c	0.9
	1200	33.5±3.1 ^b	6.4	10.6±0.5 ^a	0.24	1.8±0.03 ^a	0.21	46.4±2.1 ^b	3.1	11.4±0.2 ^d	1.3
<i>A. gibbosa</i>	350	27.8±0.5 ^a	5.3	9.0±0.1 ^a	0.20	1.7±0.01 ^a	0.20	19.0±1.8 ^a	1.3	2.7±0.5 ^a	0.3
	450	25.9±0.6 ^b	4.9	9.2±0.1 ^a	0.21	1.7±0.02 ^a	0.20	21.5±2.5 ^b	1.4	3.4±0.5 ^a	0.4
	760	28.2±0.7 ^a	5.4	9.7±0.1 ^b	0.22	1.7±0.02 ^a	0.20	52.8±6.1 ^c	3.5	7.1±0.6 ^b	0.8
	1200	28.7±0.6 ^a	5.5	9.6±0.1 ^b	0.21	1.7±0.02 ^a	0.20	85.8±11.3 ^d	5.7	9.9±0.2 ^c	1.1

591



592 **Table 4. R^2 and p-values of linear trendline of D_E versus D_{Mg} of all hyaline species of this studies**
 593 **and compiled literature studies (all studies).**

D_E versus D_{Mg}		R^2	p-value
D_{Na}	This study	0.97	<0.0005
	All studies	0.95	<0.0005
D_{Sr}	This study	0.90	<0.0025
	All studies	0.53	<0.005
D_{Zn}	This study	0.88	<0.005
	All studies	0.80	<0.01
D_{Ba}	This study	0.58	<0.05
	All studies	0.56	<0.005

594



595 **Table 5. Regression and p-values of foraminiferal Zn/Ca and Ba/Ca versus $p\text{CO}_2$ values of**
596 **different species (Fig. 4).**

Species	Zn/Ca		Ba/Ca	
	R ²	p-value	R ²	p-value
<i>M. vertebralis</i>	0.99	<0.0005	0.81	<0.025
<i>A. angulatus</i>	0.95	<0.0025	0.99	<0.0005
<i>L. bradyi</i>	0.98	<0.0005	0.97	<0.0025
<i>A. carinata</i>	0.98	<0.001	0.94	<0.005
<i>A. gibbosa</i>	0.99	<0.0005	0.98	<0.001

597